Microfluidic devices for manipulation, modification and characterization of biological cells in electric fields – a review

Jaka Čemažar[1], Damijan Miklavčič[2], Tadej Kotnik[2]

[1]College of Engineering, Virginia Tech University, Blacksburg, USA
[2]Faculty of Electrical Engineering, University of Ljubljana, Ljubljana, Slovenia

Abstract: This article presents use of electric field for manipulation of biological cells and modification of their physical properties in microfluidic chambers. Some fabrication procedures of electrodes and microfluidic chambers are presented, from thin film metal electrodes to three-dimensional structures. Strong electric field pulses induce formation of pores in cell membrane (electroporation), which allow for transport of physiologically membrane-impermeant molecules into the cell. Even stronger electric fields cause nonthermal cell lysis, which is useful in the extraction and analysis of intracellular components. Dielectrophoresis in an inhomogeneous electric field is used for manipulation of cells (e.g. guiding and patterning), characterization of their electrical properties, detection of rare cells, as well as for separation of different cells. Electroporation and dielectrophoresis can be used together on a single chip, where dielectrophoresis is used for positioning of cells where they are electroporated, which is often used for electrofusion of cells.

Keywords: microfluidic devices, electric field, dielectrophoresis, electroporation, cell separation, cell fractionation, cell fusion

Mikropretočne komore za ločevanje bioloških celic in spreminjanje njihovih lastnosti v električnem polju – zasnove, izdelava in aplikacije

Izvleček: Članek opisuje uporabo električnih polj za ločevanje bioloških celic in spreminjanje njihovih fizikalnih lastnosti v mikropretočnih napravah. Predstavljeni so različni načini izdelave elektrod in mikropretočnih naprav, od planarnih kovinskih elektrod do tridimenzionalnih struktur. V dovolj močnem električnem polju se v celični membrani pojavijo pore (elektroporacija), ki omogočijo transport molekul skozi sicer neprepustno membrano, v primeru še višjega polja pa se celica netermično lizira. Dielektroforeza omogoča premikanje in ločevanje različnih celic v nehomogenem električnem polju brez uporabe markerjev. Elektroporacijo in dielektroforezo lahko kombiniramo na čipih, ki omogočajo dielektroforetsko pozicioniranje celic in nato elektroporacijo, kar se najpogosteje uporablja za elektrofuzijo celic.

Ključne besede: mikropretočne komore, električno polje, dielektroforeza, elektroporacija, ločevanje celic, fuzija celic

* Corresponding Author's e-mail: Tadej.Kotnik@fe.uni-lj.si

1 Introduction

Electric fields can be used for manipulation of biological cells, and at sufficiently high field strengths also for modification of their physical properties.

Cells can be manipulated by *electrophoresis* (movement of charged particles in an electric field), *electroosmosis* (movement of a liquid that contains a net charge, typically close to a charged solid surface), or *dielectrophoresis* (motion of polarizable particles in an inhomogeneous electric field). Strong electric field pulses can also induce formation of aqueous pores in the cell membrane – the phenomenon termed *electroporation*, and used for transmembrane transport of molecules for which the membrane is physiologically impermeant. In addition, such pulses can also cause fusion of adjacent

cells (*electrofusion*) and non-thermal cell lysis. If the exposure and the resulting damage is sufficiently limited, the exposed cells recover and remain viable (*reversible electroporation*), while excessive damage can lead to cell death (*nonthermal irreversible electroporation*) and lysis. The electric current caused by the field can also result in Joule heating, thus exerting a thermal effect on the cells, and excessive heating leads to irreversible thermal damage.

All these effects of electric fields can also be achieved in microfluidic chambers. Small dimensions of the channels and electrodes are more suitable for working with small volumes of cell suspensions, including single cells. Microfluidic chambers for exposure of cells to electric fields are sometimes qualified among Bio-MEMS – Micro-electro-mechanical systems for biological applications. In the last years Bio-MEMS sistem were developed for many different applications for cell biology, for example cell sorting [1]–[3], formation of tissue like structures [4], [5], analysis of intracellular content [6], [7], and efects of drugs on cells [8]–[10].

In microfluidic devices due to the short distance between the microelectrodes or the electric field constriction, a low voltage is sufficient to achieve required electric field, and thus can reduce the cost of high-voltage power generators as well as the negative effect of Joule heating present in traditional systems.

In this article, we review the designs, methods of fabrication and applications of microfluidic devices for manipulation and modification of biological cells using electric fields.

2 Effects of electric fields in biological cells

2.1 Electrophoresis and electroosmosis

Electrophoresis is the motion of charged particles, relative to the liquid medium in which they are suspended, under the action of an external electric field (Figure 1a). Electrophoretic force depends on surface charge of the particle and the strength of the acting electric field. Electrophoresis is a widely used technique for separation of charged molecules and intracellular components, while for separation of cells and other methods of their manipulation it is less efficient, and thus used much less than dielectrophoresis [11].

Electroosmotic flow is the motion of a liquid that contains a net charge, typically as a result of proximity of a solid surface and formation of a double electric layer

at the interface, of which the layer of one polarity is bound to the surface, while the layer of the opposite polarity is in the liquid and thus highly mobile, so its charges are brought into motion by the field (Figure 1b). Because of the viscosity of the liquid in which the charges are dissolved, the whole liquid starts to move in the same direction. This phenomenon can be used for pumping the cell suspension into and through microfluidic devices, but generally not for finer manipulation or modification of the suspended cells [12], [13].
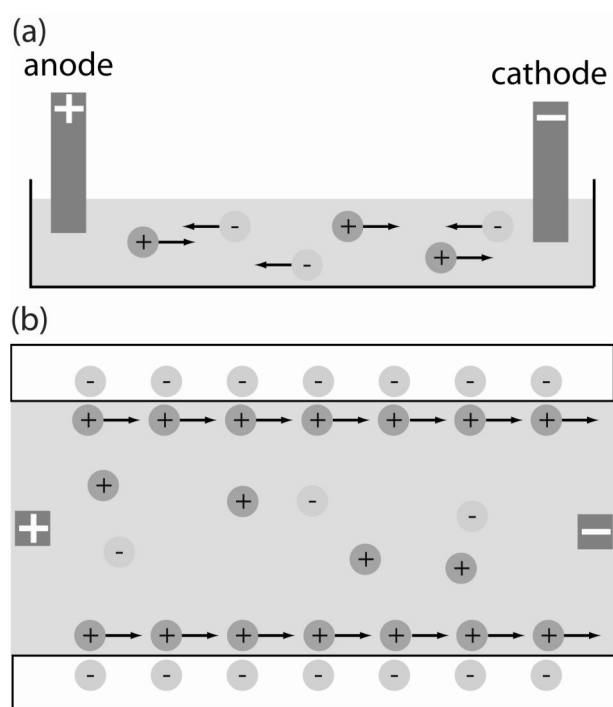

Figure 1: (a) electrophoresis, (b) electroosmosis.

2.1 Dielectrophoresis

Dielectrophoresis (DEP) is the motion of uncharged polarizable particles in a nonhomogeneous electric field [14]. An electric field induces a dipole moment of the particles, and its nonhomogeneity results in a net force on each particle (Figure 2). The size of the dielectrophoretic force (F_{DEP}) depends on the electric properties of the particles and the surrounding medium, while its direction is either towards higher field (if the particle is more polarizable than the medium – positive DEP), or towards lower field (if the particle is less polarizable – negative DEP).

Common uses of dielectrophoresis when applied to biological cells are in selective manipulation (e.g., focusing, guiding, and/or patterning) [15], [16], in separation of two or fractionation of several different cell groups [17], and in characterization of their properties [18]. Electrically, the cell plasma membrane represents a thin insulating sheet surrounded on both sides by
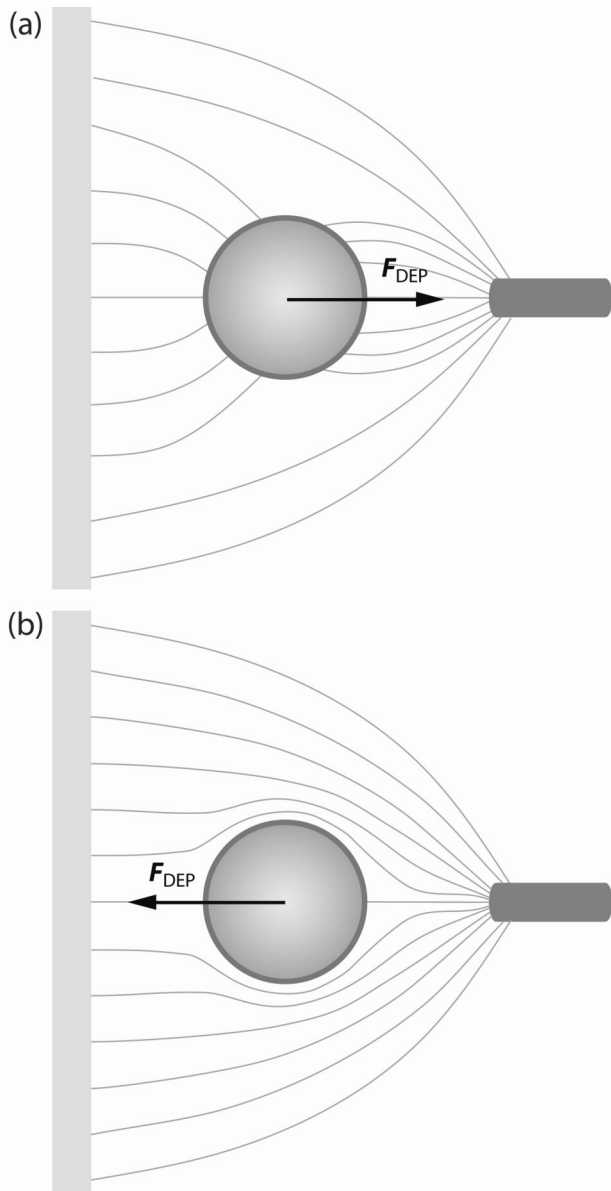
Figure 2: Dielectrophoresis: (a) positive, (b) negative.

aqueous electrolyte solutions. Time average of dielectrophoretic force acting on a spherical cell enveloped by a single membrane (i.e., a single-shell model of a cell) in an alternating electric field with amplitude E and angular frequency ω is given by [19]

$$F_{DEP} = \pi\varepsilon_0\varepsilon_e r^3 (\mathrm{Re}[f_{CM}(\omega)]\nabla|E^2| +$$
$$+ 2\,\mathrm{Im}[f_{CM}(\omega)](E_x^2\nabla\varphi_x + E_y^2\nabla\varphi_y + E_Z^2\nabla\varphi_Z))' \quad (1)$$

with f_{CM} denoting the Clausius-Mossotti factor expressed as

$$f_{CM} = \frac{\varepsilon_c' - \varepsilon_e'}{\varepsilon_c' + 2\varepsilon_e'} \quad (2)$$

and with

$$\varepsilon_c' = \varepsilon_m' \frac{\left(\dfrac{r}{r-d}\right)^3 + 2\dfrac{\varepsilon_i' - \varepsilon_m'}{\varepsilon_i' + 2\varepsilon_m'}}{\left(\dfrac{r}{r-d}\right)^3 - \dfrac{\varepsilon_i' - \varepsilon_m'}{\varepsilon_i' + 2\varepsilon_m'}} \quad (3)$$

where r is the cell radius, d is the membrane thickness, φ is the phase delay between the components of the field, and ε_e', ε_m', and ε_i', are the complex dielectric permittivities of the external medium, membrane, and the cell interior (cytoplasm), respectively, each given by ε' = ε – iσ/ω, with ε and σ the dielectric permittivity and the electric conductivity of the region, and ω again the angular frequency of the field.

The second term (summand) in Eq. (1) is non-zero only if a system of multiple electrodes is used and there is a phase delay between the field-generating signals delivered to them; this type of cell manipulation is termed *travelling-wave dielectrophoresis* [20]. If such electrodes are positioned in a radially symmetrical manner, and the signals are delivered as to generate a rotating electric field, this results in circular motion of the cells in the region between the electrodes, termed *electrorotation* [19].

But more typically, only one pair of electrodes is used, so that Eq. (1) simplifies into

$$F_{DEP} = \pi\varepsilon_0\varepsilon_e r^3 \,\mathrm{Re}[f_{CM}\omega]\nabla|E^2| \quad (4)$$

with Eqns. (2) and (3) still valid. These equations show that at a given electric field, F_{DEP} is proportional to the real part of f_{CM}, which itself is a function of the field frequency, and this function will henceforth be referred to as the *dielectrophoretic spectrum* (*DEP spectrum*).

Separation of cells by dielectrophoresis is therefore possible if the cells in the mixture belong to two (or more) populations, each with either a different geometry, or different electric conductivity and/or dielectric permittivity [20]. Different geometrical and electrical properties result in different dielectrophoretic force acting on the cells of each population. Separation is the most successful if the two populations of cells to be separated differ in their crossover frequency (frequency of transition between negative and positive dielectrophoresis), and the applied field frequency is chosen in the manner that one population is subject to negative, and the other to positive dielectrophoresis, so that the dielectrophoretic force acts on them in opposite directions.

2.2 Electroporation

An exposure of a cell to a sufficiently high external electric field results in electroporation – formation of nanoscale aqueous pores in the lipid bilayer of the cell plasma membrane [21]–[24]. These permeable structures provide a pathway for diffusive transport of otherwise membrane-impermeant molecules into and out of the cells. If the exposure is sufficiently short and the membrane recovers sufficiently rapidly for the cell to remain viable, electroporation is reversible, otherwise it is irreversible.

Reversible electroporation is already an established method for introduction of membrane-impermeant chemotherapeutics into tumor cells – *electrochemotherapy* [25], and a promising technique for gene therapy devoid of the risks caused by viral vectors – *gene electrotransfer* [26]. In medicine, irreversible electroporation is a method for tissue ablation – *nonthermal electroablation* [27], while in biotechnology it is used for *electroextraction* of biomolecules [28] and microbial deactivation, particularly in food preservation [29] (Figure 3).

The voltage on the membranes of the exposed cells, termed the *induced transmembrane voltage (ITV)*, represents a part of the voltage delivered to the electrodes and is position dependent; thus in spherical cells, it varies proportionally to the cosine of the angle θ measured from the center of the cell between the position on the membrane and the applied field direction [30]

$$\mathrm{ITV} = \frac{3}{2} ER\cos\theta$$

(5)

The ITV thus has extremal values at the points where the field is perpendicular to the membrane, i.e., at θ = 0° and θ = 180° (the "poles" of the cell), and is zero at 90° (the "equator"). Thus, if the peak transmembrane voltage of 0.3 V is to be achieved on a cell with a 10 μm radius, the cell has to be exposed to a field of about 200 V/cm.

2.3 Electrofusion

Cell fusion is a method for achieving nucleus transfer, hybridoma and epigenetic reprograming of somatic cells. Fusion of two different types of cells generates a third, polynuclear type that displays hybrid characteristics of the two parental cells (Figure 3). Although chemical (polyethyleneglycol treatment) or viral methods can be used for cell fusion, electrofusion is safer, more controllable and it can provide high yield of fused cells [32], [33].
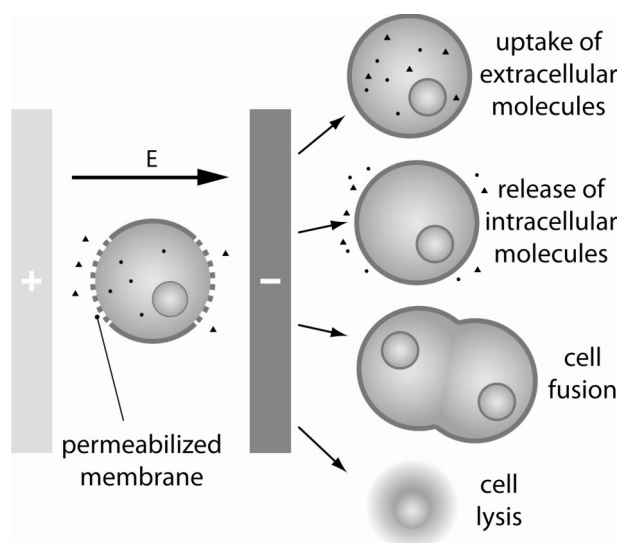

Figure 3: Use of electroporation: transport of molecules across the membrane, cell fusion and cell lysis. Adapted from [31].

For fusion, cells must be brought into a close contact, which can be achieved by chemical methods, sedimentation, in microstructures or by dielectrophoresis [34]. Traditional bulk pairing methods are mostly nonspecific, so that from a mixture of type A and type B cells one gets hybrids of AA, BB, and AB types, while generally only the latter are desired. Specific pairing methods, which are best achieved in microfluidic chambers, can increase the yield of the desired hybrid type.

Once the contact is achieved, electric pulses can be used to bring the membranes in contact into a fusogenic state, and thus facilitating the fusion of the two cells into a single hybrid cell [34].

3 Fabrication of microfluidic devices

Fabrication of microfluidic devices is often based on processes developed and used in semiconductor industry. The most frequently used materials are silicon, glass and gold. However, the cells suspended in fluid media introduce specific requirements that have lately led to an increasing use of plastics. Chambers are typically transparent, which allows for observation under the microscope, they have inlets and outlets for fluid flow. The electrodes are most often in direct contact with the cell suspension, and thus for every new experiment, the chamber must either be thoroughly cleaned, or replaced by a new one.

In the design of microfluidic devices, the designer must simultaneously consider the specifics of the fluid flow, electric field distribution, electrode fabrication, and

encapsulation. Modeling of such devices therefore requires knowledge of several different areas of physics, and verification of such models can be difficult, particularly as the electric field strength and its distribution within the chamber cannot be measured directly. Standardization of dimensions, which would allow for interconnection of several devices into a more complex system, is currently poor, as some chamber dimensions are adopted from semiconductor industry (e.g., silicon or glass wafers), and others from cell laboratory equipment (e.g., microscope slides and microtiter plates).

In the last years, a trend of standalone *lab-on-a-chip* or *µTAS* (micro total analysis) devices has started to emerge. The goal is to make small portable devices into which a sample of cells can be loaded, and all of the requested information extracted. However, current systems mostly still require connection of these small devices to external pumps, large electrical signal (function) generators, centrifuges, and often also manual pre- and post-handling of liquids and cells.

For analysis, small size is a great advantage, because very small amounts of stains or other expensive chemicals are required. In contrast, for production of cells with desired properties (for example production of cell hybrids by means of fusion), small volumes and thus small yields are a disadvantage. As microdevices often cannot be scaled up in all dimensions, particularly due to the loss of control of individual cells and the impact on the surface-to-volume ratios, designers must in such cases rely on parallelization.

3.1 Bio-MEMS materials

Desired Bio-MEMS materials are biocompatible, chemically modifiable, easy to fabricate, economic, soft and flexible. The most often used materials are borosilicate glass, silicon, gold, indium-tin oxide (ITO), titanium, chrome, silicon dioxide, silicon nitride, silicon carbide and polymers poly dimethyl siloxane (PDMS), poly methyl methacrylate (PMMA), SU-8 epoxy photoresist, and polyimide [35], [36].

Generaly used materials and fabrication processes of microfluidic devices were reviewed elsewhere [5], [6], [37], here we describe fabrication of typical microfluidic device prototypes for cell manipulation and modification by elecric field.

Borosilicate glass is widely used as a base plate for microfuidic devices. It is chemically resistant to liquids used for suspending cells, it is highly transparent for broad range light wavelengths (~300-2200 nm), it is suitable for deposition of metallic and polymeric layers, and it can withstand high temperatures during metal deposition process. It can be anodically bonded to silicon, and fluidic channels can be made by etching. Thickness of the glass wafer is typically less than 1 mm, due to which large microchambers are brittle. Polymers are more flexible, for example polyimide can be used as the bottom plate for large electrode deposition [38]. PDMS is most often used as a cover or part of the chamber. It can be easily molded and cured and it is optically transparent, flexible, it has very low electric conductivity and it is biocompatible. It is also inexpensive and therefore a new chamber can be made for every experiment if required. Molds for PDMS chambers are typically made from silicon wafers by patterning SU-8 [39] or by etching in silicon by deep reactive ion etching (DRIE), which is more durable, useful for high aspect ratio structures, but more expensive [2].

Stainless steel is sometimes used for larger parts of microfluidic chambers, but not for smaller structures, as these are difficult to fabricate, and it is also preferable to avoid it in electrodes used for delivery of strong electric pulses, as electrolytic release of Fe^{2+} and Fe^{3+} ions can contaminate the cell suspension [40], [41]. Aluminum is sometimes used as an alternative; this similarly results in release of Al^{3+} ions, but the release was reported to be lower when using short pulses (≤ 100 µs) [41], [42]. The most expensive solution, but least problematic from the aspect of electrolytic contamination, is to construct electrodes from platinum.

Silicon is mechanically strong, and many techniques for fabrication of silicon microelectronic structures have been developed, making it a common material in microchamber fabrication. Silicon derivatives such as SiO_2, Si_3N_4 and SiC are insulators, which allows for construction of multilayer structures. The electrical conductivity of pure silicon is low (~10^{-4} S/m), but it can be increased by many orders of magnitude (up to 10^5 S/m) by doping the silicon substrate with conductive atoms [43]. Gold offers an even higher electrical conductivity, and higher chemical inertness than doped silicon, but it is typically only depositable in thin layers (up to 250 µm), while thicker layers are difficult to fabricate.

ITO is a conducting material, which is optically transparent in thin layers. Polymers can also be made conductive my mixing them with small conductive particles of silver or carbon. When concentration of these particles reaches the percolation threshold, electric current can flow through a mesh of these particles and electrical conductivity is increased by several orders of magnitude. As the volume of silver particles in PDMS reaches 19%, conductivity increases almost stepwise from $2.5 \cdot 10^{-14}$ S/m to $6.2 \cdot 10^3$ S/m [44], while addition of carbon black powder to PDMS can increase its conductivity up to 15 S/m [45]. Mechanical properties of

polymers with added particles are not altered as much as electric conductivity. A disadvantage of using non-metal electrodes is the need to use higher voltages to generate the same strength of electric field in comparison to metal electrodes. For dielectrophoresis and electroosmosis between the electrodes not more than 100 µm apart, the voltage of ±5 V is often sufficient, and common function generators can be used for this purpose. For higher voltages, amplifiers or custom built generators are required.

Cells tend to form clusters, and also bind to some surfaces, especially to metal electrodes. To prevent such binding, the internal surfaces of the chamber can be coated with antifouling molecules, such as Bovine serum albumin or polyethylene glycol [46].

3.2 Assembly, fluidic and electric connections

Assembling Bio-MEMS devices requires not only electrical, but also fluidic connections, and designing the shape of the channels and their assembly is as important as designing the appropriate shape of the electrodes [35]. Fluidic connections to flexible PDMS chambers can be made by punching PDMS device before bonding and inserting appropriate size tubing into holes. For rigid materials such as glass and silicon fluidic connectors holes must be drilled or etched and commercially available fittings can be used to connect tubing [47], [48]. For electrical connections part of metal layer must be uncovered or holes must be drilled to cover plate [47], [49]. Chamber components must be sealed in a watertight manner to prevent leakage, but if they are not for single use, they must at the same time allow for cleaning and/or replacing parts. Thus, parts of single-use chambers can be permanently glued or bonded together (glass-glass or glass-silicon bonds), while reusable chambers must allow for disassembly either by pressing the parts together with an external frame and sealing the contacts temporarily with a soft material (rubber, wax), or by weak bonding (plasma activation of PDMS and bonding to glass).

3.3 Fabrication techniques

For fabrication of large number of devices, plastic is the material of choice, while for prototypes and devices made in low production quantities, fabricated glass with thin metal film is often chosen due to precision and reproducibility of fabrication, as well as of the electrical and chemical properties of the materials (Figure 4a). Pyrex glass is thus used as a basis for the electrodes onto which a layer of metal (chromium, titanium or gold) is deposited by chemical or physical (sputtering) vapor deposition. Thickness of the metal film is typically several hundred nm. Then, the photoresist layer is spun-on onto metal-covered substrate surface. The chosen pattern of the electrodes is transferred onto photoresist by illuminating through the mask (photolithography). This process is followed by wet or dry etching of thin metal layers on the part of the surface not protected by photoresist, and concluded by cleaning the remaining photoresist. For three-dimensional structures deposition of photoresist, photolithography and etching can be repeated. Thick layer of metal can be deposited over thin film by electroplating; however, photolithography of thick photoresist is done before electroplating, and fluidic channels are formed by removing the remaining photoresist [35].
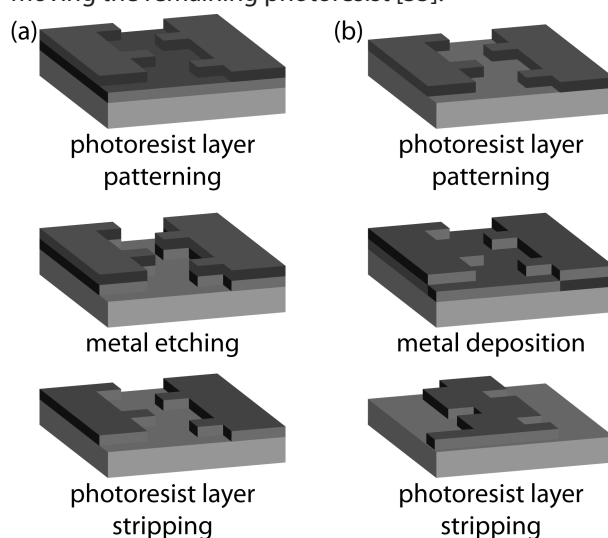

(a) photoresist layer patterning · metal etching · photoresist layer stripping

(b) photoresist layer patterning · metal deposition · photoresist layer stripping

Figure 4: Fabrication of thin film electrodes. a) etching into metal layer, b) lift-off process. Adapted from [36].

Electrodes for MEMS can also be made by a lift-off process (Figure 4b). Photoresist is deposited on glass wafer, patterned by photolithography, and then a layer of metal is deposited, for example with electron beam evaporation. Finally, the photoresist is chemically removed and metal layer remains only on the part of the surface that was not covered by photoresist.

Laser ablation is another technique used to make electrodes from thin metal film. A thin metal film is deposited on a glass substrate. A laser beam heats a small volume of the metal, causing evaporation. By guiding the laser over the substrate, the required pattern is formed. The advantage of this process is in the absence of mask and etching, while its disadvantage is in the rougher surfaces and edges, and it is mainly used for fabrication of prototype devices.

Chambers with three-dimensional electrodes are typically made of insulating materials, which can easily be deposited in layers with thicknesses over 10 µm (thus exceeding the dimensions of biological cells), and with the deposition followed by electroplating of metal.

Fabrication of three-dimensional structures from silicon is well-established, but for electrodes, silicon must be heavily doped to attain sufficient electrical conductivity (at least 1 S/m [47]). The chamber can be made transparent if the electrodes are made from silicon on glass wafer and anodically bonded to the glass plate on top of the channel. The holes for fluid connections are drilled or etched into the glass. Channels more than 100 μm deep can be formed by deep reactive ion etching (DRIE). By exchanging etching and passivation (Bosch process), vertical sidewalls are formed, with very high reproducibility of the process [47].

The LIGA process (from German: Lithographie, Galvanoformung, Abformung) is used for fabrication of thick three-dimensional structures. A thick layer of photoresist is deposited on a conductive plate, and a pattern of electrodes is transferred to this layer by illumination through a mask (photolithography). Then a layer of metal is deposited in the gaps in photoresist, and the remaining photoresist material is cleaned. The result are thick metal electrodes that can also be used as a mold for injection molding of plastics. The disadvantage of this process is the required use of a high-power beam source of parallel X-rays when illuminating through the mask, and a synchrotron is generally required to generate this beam [36].

Inhomogeneous electric field for dielectrophoresis can be generated also by placing insulating structures into an otherwise homogeneous field – *insulator dielectrophoresis* (iDEP). Electric field is still generated by metal electrodes, but the electrode shape can be much simpler. Thin-layer metal electrodes positioned along the channel, or even a pair of wires can be used. To achieve the field nonhomogeneity, insulating structures such as constrictions or pillars are formed between the electrodes, e.g. by isotropic etching in glass [25]. A layer of chromium is deposited on the glass mask, serving as hard mask. Then a layer of photoresist is deposited, patterned and developed. Exposed chromium is etched and subsequently, the exposed glass is etched with a solution of hydrofluoric acid. The plate with the channel is bonded to the cover plate, forming a chamber. Another option is creating a mold and then using an injection molding process to create a channel from polymer material [50].

An alternative way of creating electrodes for dielectrophoretic separation are optoelectric tweezers [51]. A photosensitive layer consisting of n+ a-Si:H, intrinsic a-Si:H, and SiC$_x$ films is deposited over a layer of indium-tin oxide (ITO) on glass. The photosensitive layer becomes electrically conductive when illuminated. By selectively illuminating this layer through a mask or by an adequate projector, virtual electrodes are generated that only remain conductive for the time of illumination. By applying AC voltage onto these electrodes, the cells can be manipulated or separated by means of dielectrophoresis. The advantage of such electrodes is their easily changeable shape, and a much lower density of the light current in comparison to optical tweezers. Their weakness is considerably lower electrical conductivity of virtual electrodes in comparison to metallic ones, due to which dielectrophoresis only functions with cells suspended in a medium with a very low electrical conductivity.

4 Applications of microfluidic devices

4.1 Electroporation

In traditional electroporation devices, hundreds of μl of a cell suspension (typically corresponding to millions of cells) are exposed to electric pulses simultaneously. To achieve electroporation, voltage in hundreds or even thousands of volts must be delivered to the electrodes, and special safety precautions are thus required. The large exposed volume can also contain local nonhomogeneities of the field, and consequently variable rates of porated and surviving cells, as well as variations in the local pH. Aluminum and stainless steel typically used for electrodes in such devices are sources of electrolytic contamination of the suspension with metal ions [41], with possible unpredictable effects on cells.

Microfluidic electroporation devices overcome many of the abovementioned shortcomings of conventional (bulk) electroporation, and add several other advantages [52]–[57]. Since electroporation in such devices is performed with a much narrower gap between the electrodes, several volts suffice for electroporation, and safety precautions can be avoided, lowering considerably also the power consumption and heat generation. At the same time, the small gap relative to the area of the electrodes also assures a high homogeneity of the field, and also largely reduces the electrolytic contamination, as well as the variations in the local pH [53]. In microscale devices, the larger surface-to-volume ratio also leads to the faster heat dissipation, making it possible to distinguish between the heating effects and the electric field effects, which is yet another advantage of microfluidic electroporation devices.

While the limited processing volume can be viewed as a shortcoming of microfluidic electroporation, this can largely be overcome by performing electroporation in a continuous flow [58]. Microfluidic electroporation also offers the possibility of real-time monitoring and visualization of cellular and intracellular response to

the electric pulses (using fluorescent probes for example), including molecular uptake.

The ability to perform single-cell electroporation is another advantage of the microfluidic electroporation, particularly from the aspect of basic research. Namely, it is possible to trap a single cell in a specific location within the microfluidic chamber, and then study effects of electric pulses under a high-magnification microscope, which is almost impossible to achieve in volumes used with conventional electroporation equipment. Microfluidic electroporation devices also offer high potential for integration with other microfluidic components to form a multifunctional lab-on-a-chip system, which would greatly facilitate biochemical experiments consisting of several stages.
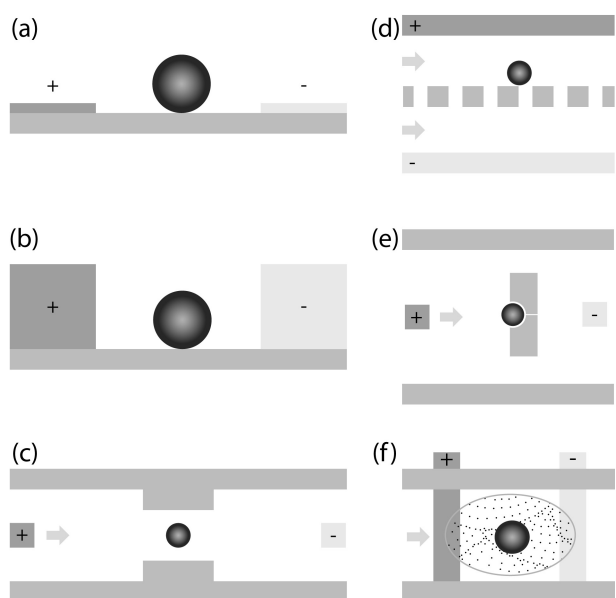
Figure 5: (a) thin film metal electrodes, (b) thick metal electrodes, (c) electroporation in a channel with constriction, (d) electroporation on an insulating mesh/between pillars, (e) electroporation of cells trapped on insulating structures, (f) electroporation in aqueous droplet in oil. Panels (c-f) adapted from [59].

4.2 Gene electrotransfer

For cell transfection (transfer of genetic material into the cell and subsequent gene expression), electroporation must be well controlled to ensure cells are sufficiently electroporated, yet they remain viable. Microfluidic chambers allow for exposure of a single cell or a bulk of cells to electroporative pulses. Cells can flow though the chamber where they are electroporated either sequentially, or simultaneously in several designated positions. Electroporation is preferably performed in a homogeneous electric field using rectangular electric field pulses, but if cell positioning is well

controlled, an overall nonhomogeneous field can also be suitable for the task.

For transfection of molecules into single cells, Valero et al. [60] used a microfluidic device with two channels etched into silicon by reactive ion etching. For positioning of single cells between the electrodes, a hole in the wall between two channels was etched. This allowed the fluid to flow through the holes, but not the cells for which the holes were too small. Channels were covered with glass on which platinum electrodes were sputtered prior to anodic bonding to the silicon wafer. When cells were trapped, DNA plasmid was released into the medium surrounding the cells, and the cells were individually electroporated. Transfection rate of 75% was achieved, which is quite high compared to typical yields with electrotransfer performed in bulk suspensions.

Vassaneli et al. [61] used an array of 60 cell-sized microelectrodes that enabled single-cell electroporation of attached cells. This silicon microchip was fabricated using the backend of a CMOS (complementary metal–oxide–semiconductor) process. The active area of the electrodes was made of a gold layer, and its diameter ranged between 15 and 50 µm to match different sizes of different cell types. The chip was encased with a plastic culture chamber, and the electrodes were individually addressable by the switching system.

Many cells can be electroporated and transfected in a simple microfluidic PDMS channel between two reservoirs with two platinum wires as electrodes. Traditionally, the direction of electric field is perpendicular to the flow direction, but orienting the electric field along the channel allows for much easier fabrication, as the channel can be made from a single insulating material, and the electrodes can be simple wires. Moreover, the ratio between electrodes surface and suspension volume is much smaller than in the case of metal electrodes positioned along the channel. Voltage drop on the electrode-liquid interface is relatively small due to the large distance between electrodes. Two reservoirs can be connected with many channels, which allows for simultaneous electroporation of cells in all the channels. Such channels can have different lengths, making the electric field in each channel different, which is particularly useful for determining e.g. the threshold electric field strength for electroporation [62].

The electric field between two reservoirs can be concentrated (focused) by positioning an insulating constriction into the channel (Figure 5c). By adjusting the frequency of electric pulses and flow rate, the operator determines the number of pulses to which each cell is exposed. Only one cell at a time can be inside the constriction, as other-

wise the cells would be exposed under different conditions. If the time spent by a cell inside constriction is very small (a few ms), a continuous DC voltage can also be used for electroporation. Wang et al. [63] made a channel 7 mm long, 213 μm wide, and ~33 μm high in PDMS, containing in its middle a narrower channel 2 mm long and 33 μm wide. Electric field inside the constriction was thus 5 times stronger than outside it. A mold for this chamber was fabricated using soft lithography on a layer of SU-8, and then PDMS was poured on it and cured. After removing the mold, the surface of PDMS was oxidized and bonded together with the glass slide. Platinum wires were used as electrodes.

Zhan et al. [64] used a similar channel, but with four constrictions (the equivalent of exposure of cells to four pulses), obtaining electroporation of CHO cells with transfection rate of 30 %. This type of devices allows for high-throughput controlled electroporation and transfection of cells flowing through the channel. Required voltage between electrodes was a few hundred volts and the cells had to be suspended in low-conductivity buffer to avoid thermal damage to the cells. Fabrication of such devices is relatively simple, but the chambers are for single use.

Electroporation in a channel with small electrode surfaces can be performed on a chip with a salt bridge. Kim et al. [53] developed such an electroporation chip made of PDMS channels on a glass. The mold for PDMS casting was made of SU-8 on a silicon wafer. Cells flowed through the main channel, while two side channels were filled with hypertonic hydrogel with conductivity of 16 S/m. Side channels were connected with the main channel through small openings, and the hydrogel delivered most of the applied voltage to the main channel, with the electric field focused in the low-conductivity cell suspension. The advantage of a salt bridge is absence of bubble generation and of electrolytic decomposition present on metal electrodes, since Ag-Ag/Cl electrodes are in direct contact only with the salt bridge. With a 10 V DC input voltage delivered to the chip, electric field in the main channel reached 900 V/cm.

The most straightforward method for decreasing required voltage for electroporation is to reduce the distance between the electrodes. Channels made in a single thin film layer cannot provide homogeneous electric field, since cells are larger than the layer thickness, but bonding together two plates, each with its own thin metal layer, so that they face each other, forms a channel with homogeneous electric field suitable for continuous electroporation. Lin et al. [65] fabricated such a chip using thin film evaporation, photolithography, lift-off process and fusion-bonding methods. A PMMA plate (Poly methyl methacrylate known as acrylic glass) was used for the top and the bottom plate, each with a layer of Au/Ti electrodes. A groove was precisely cut on a piece of PMMA substrate using an excimer laser and all pieces were fused together. The channel was 0.2 mm high, 5 mm wide and 25 mm long. With 10 ms rectangular pulses of 10 Hz frequency and 10 V amplitude, 500 V/cm electric field was generated. The authors obtained electrotransfer of the GFP gene, but did not report the transfection rate.

Zhan et al. [66] developed a microfluidic device that encapsulates cells into aqueous droplets and then electroporates the encapsulated cells. The device was fabricated based on PDMS using the standard soft lithography method. Thin film Au electrodes were fabricated on glass and PDMS was bonded with glass to form a chamber. A simple T-junction channel was used to produce droplets of monodispersity. For electroporation, a constant voltage was established across a pair of microelectrodes on the glass substrate in the downstream. The droplets with cells flowed continuously through the microelectrode pair, and because the oil phase is nonconductive, each flowing buffer droplet experienced a field intensity variation equivalent to a pulse with duration equal to the time during which the two electrodes were connected by the droplet. The microfluidic electroporation approach based on droplets could reduce the volume of dyes or reagents used for analysis, although the mixing of droplets with oil decreased the viability of cells by about 11%, which is significant but not critical for most of the applications.

Macqueen at al. [67] proposed electroporation in a nonhomogeneous electric field in combination with dielectrophoretic positioning. Thin Ti/Pt electrodes were fabricated on glass slide using standard lift-off processes. Surface of the electrodes was covered with a thin 50 nm layer of coatings using plasma-enhanced chemical vapor deposition. Electrically insulating (SiN_x:H) barriers prevented electrolysis of the suspension medium. A function generator provided both the AC field for dielectrophoretic positioning, and the pulses for electroporation. Such a device is very versatile, and can in principle be used for applications ranging from observation of dielectrophoretic separation of cells, measurement of crossover frequency, electrorotation, dielectrophoretic deformation, to transfection or cell lysis. As a disadvantage, such a chamber is suboptimal for any of these procedures from the aspect of achievable efficiency.

4.3 Cell lysis

Large devices for cell inactivation are typically used in industry for food preservation or deactivation of microor-

ganisms in water. They are most often made from stainless steel pipes (tubes). However, for studying the process of cell lysis, much smaller and transparent chambers are required, so that the effects can be monitored under the microscope. The advantage of cell lysis achieved with electric field pulses, in comparison to chemical lysis, is that only the outer cell membrane is damaged, while the organelle membranes remain intact.

Huang and Rubinsky [68] fabricated the first microfluidic devices capable of electroporating single cells. It had a multiple-layer chamber, consisting of three chips glued together placed on acrylic substrate with fluidic connections. Materials used for chamber fabrication were n-type silicon, silicon nitride, silicon dioxide and aluminum. For fabrication, standard silicon microfabrication technology (photolithography, etching) was used. Electrodes were in the top and the bottom layer, and in the isolation layer between them a 2 µm diameter hole was drilled. The cell was positioned on the hole, where the electric field was the strongest. The cells could be electroporated either reversibly or irreversibly with this device. By monitoring the electric current it was possible to detect the presence of the cell on the hole and deliver the electroporating pulse accordingly.

A chip with thick electrodes for cell lysis was fabricated by Lu et al. [69]. Glass substrate was covered with thin layer of gold. A thick layer of SU-8 was deposited, patterned and then additional thick layer of gold was electroplated. Then SU-8 was removed and deposited again with the pattern of a microfluidic channel. On the top of the channel cover slip was glued with epoxy. The device was used for lysis of human carcinoma cells. At 10 V of AC voltage delivered to the electrodes, a nonhomogeneous field in the range of kV/cm was generated. Nonhomogeneous fields formed around such electrodes generates positive dielectrophoresis, so that the dielectrophoretic force pulls the cells into the region of the highest electric field, where they are irreversibly electroporated [70], [71].

4.4 Measuring cell properties by dielectrophoresis and electrororation

Microelectrodes can be made in various shapes on a single chip, allowing for studying multiple effects of the electric field [16], [72]–[76]. For example, Müller et al. [72] constructed a three-dimensional microelectrode system for handling of single cells. It was designed to focus, trap and separate cells using negative dielectrophoresis, and they used two different systems. The first was fabricated by laser ablation of thin platinum layer on glass, with a polymer sheet used as spacer and two glass surfaces with electrodes assembled together

face-to-face. The second system was fabricated with standard photolithography and lift-off process on glass with thin platinum layer and also assembled in a microfluidic chamber. When the cells entered the chamber, they were dielectrophoretically aligned in the middle of the channel, then individually measured by electrorotation and finally sorted in two channels by dielectrophoretic force. Such systems can operate continuously, but the throughput is low.

Cen et al. [73] combined dielectrophoresis, traveling-wave dielectrophoresis and electrorotation on a single chip. Planar microelectrode array was manufactured using CMOS process technology. It had two metal layers, one layer are electrodes and one layer for electric connections of bonding pads and electrodes. Conductive ITO glass was used as cover forming a microfluidic channel. Concentric circles were used for levitation, and the dielectrophoretic force was adjusted to provide equilibrium with sedimentation force. Electrodes for traveling-wave dielectrophoresis were concentric circles with phase-shifted sine voltage delivered to them, so that the cells were moving radially between these electrodes. Electrodes for electrorotation consisted of four sets of electrodes with phase-shifted signals forming a rotating field. Measurement on Daudi and NCI-H929 cells showed that viable and nonviable cells have different capacitance of the cell membrane.
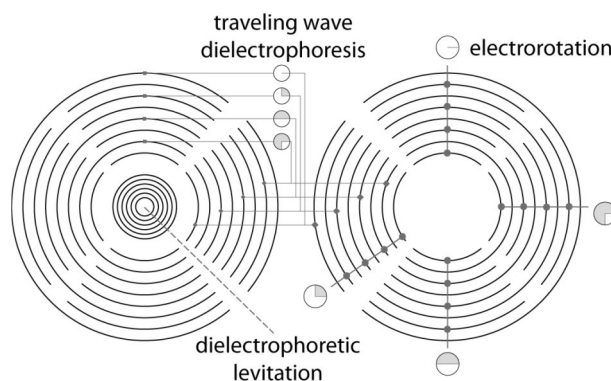

Figure 6: Electrodes for measuring cell properties by dielectrophoretic levitation, traveling wave dielectrophoresis and electrorotation. Adapted from [73].

4.5 Separation and fractionation of cells

For dielectrophoretic separation into two or fractionation into several subpopulations of cells, nonhomogeneous electric field is required. It can be generated using two different approaches – either by suitably shaping the electrodes, or by placing insulating structures into an otherwise homogeneous field generated by plate electrodes. In this section we present a concise overview of such devices and their use for dielectrophoretic separation and fractionation, while many fur-

ther details can be found in several comprehensive reviews that have been published recently [16], [77]–[82].

Typical shapes of planar thin-film electrodes are shown in Figure 7. They can be interdigitated [74], [83]–[85], castellated [86], curved [87], quadrupolar [15], or forming microwells [79]. These electrodes produce electric filed gradient both in the plane of the electrodes and perpendicularly to this plane.

Three-dimensional electrodes, some of which are shown in Figure 7, provide a better definition and control of the electric field and its gradient, but are generally more difficult to fabricate. In such designs, the chamber can be constructed from electrodes deposited both on the top and the bottom plate [88], or metallic posts can be extruded [89], or deposited in a thick layer by electroplating, thus forming vertical sidewalls [90]. The electrodes for generation of dielectrophoretic force can also be simple wires in reservoirs (similar to those in some electroporation chambers), with insulating pillars in the channel between the electrodes [91].
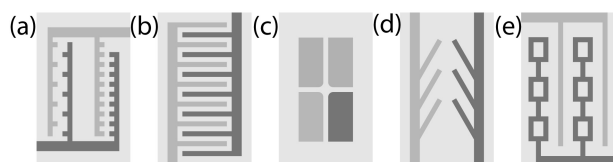

Figure 7: Classification of planar electrodes: (a) castellated, (b) interdigitated, (c) quadrupolar, (d) oblique, (e) microwells. Adapted from [79].
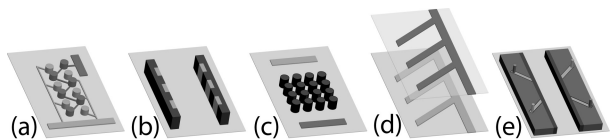

Figure 8: Classification of three-dimensional electrodes: (a) extruded, (b) sidewall patterned, (c) insulator-based, (d) top-bottom patterned and (e) contactless. Adapted from [79].

Many different strategies for cell separation can be used. Voldman et al. [89] describe a cell trapping method in a chamber with extruded metal electrodes, as shown in Figure 8a. For this method, a batch of cell suspension is injected in the chamber, and if two types of cells differ in their properties sufficiently, and an adequate field frequency is chosen, one type of cells from a mixture is trapped on the electrodes by positive dielectrophoresis, while the other type is repelled from them, flowing through the chamber. As the electric field is switched off, the trapped cells are released and also start flowing towards the output of the chamber.

Trapping of cells is also possible by negative dielectrophoresis on thin microwell electrodes, as shown in Fig-

ure 7e [92]. Here, one type of cells is immobilized in the center of the microwell, while other cells flow through the chamber. In contrast to trapping by positive dielectrophoresis, the cells are not exposed to high electric field, but the throughput is rather low.

Higher throughputs are achievable in chambers in which the dielectrophoretic force is used to change the trajectory of cells flowing through the channel. Han and Frazier [93] designed electrodes for lateral separation oriented at oblique angle according to fluid flow (Figure 7d), so that the dielectrophoretic force pushes the cells laterally either towards the center, or towards the sides of the channel. Their chamber has three output channels through which the separated cells leave the chamber and can be collected into three separate containers. Golden electrodes were deposited on glass with standard photolithography and the channel was made of PDMS bonded to glass. The device was used for separation of white and red blood cells, yielding samples of 92 % and 87 % purity, respectively.

Lewpiriyawong et al. [94] fabricated PDMS-based microfluidic device with sidewall AgPDMS electrodes. Along one side wall of the main channel 200 μm wide and 40 μm deep, there are four 100 μm wide AgPDMS electrodes, spaced 100 μm apart. This chamber was fabricated by patterning SU-8 on silicon wafer to create cavities for housing AgPDMS. Conducting paste (AgPDMS) with an electrical conductivity of ~2 ×10^4 S/m was made by mixing 1 μm silver (Ag) particles with PDMS gel at a ratio of 85% w/w is filled into cavities. Channels were formed by molding PDMS and device was bonded to glass. This chamber, illustrated in Figure 9, has two inlets and two outlets. The cell suspension thus enters the chamber from one channel, while the other input channel is used for hydrodynamic focusing of cells. When the cells flow near the electrodes, they are either attracted to them or repelled from them, depending on the sign of the dielectrophoretic force. Separated cells are leaving the chamber continuously through two channels. This device was found useful for determining the cells' crossover frequency, as well as for separation of living and dead yeast cells, with efficiency of 97 % [94].
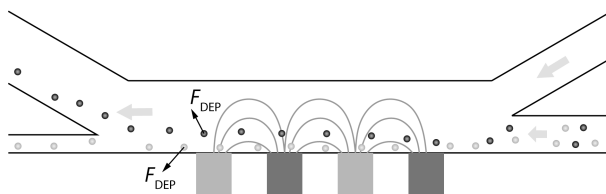

Figure 9: Dielectrophoretic separation with lateral "shift" of trajectories of cells. Adapted form [94].

Typically, the cells are separated by the sign of dielectrophoretic force, whereas separation by the magni-

tude of this force leads to separation by cell size due to its very strong dependence on cell size (proportional to r^3). Separation by other parameters is difficult, but the influence of cell size is decreased in dielectrophoretic field-flow fractionation (DEP-FFF) chambers, where separation is based on the balance between dielectrophoretic and gravitational force, which are both proportional to r^3 [95], [96]. Such chambers contain a long shallow channel with thin interdigitated electrodes at the bottom which create an electric field nonhomogeneous mainly in the vertical direction. At a properly selected frequency, the dielectrophoretic force pushes cells up, while sedimentation force pulls cell down. As the dielectrophoretic force decreases with the increasing distance from the electrodes, each cell reaches its steady-state position at a specific vertical position where the two forces are in equilibrium. The fluid flow in the shallow channels is laminar and has a parabolic velocity profile in vertical direction, so that the cells flowing at the bottom and the top of the channel flow through the chamber at the slowest rate, and the cells at the middle height flow the fastest. Due to different flow rates, vertical separation leads to horizontal separation along the channel, and allows for continuous separation if the chamber has two outputs at different vertical positions, and for batch separation if there is a single output, and the cells are collected into different containers at different times elapsed after the cells are injected at the channel's input. In this manner, DEP-FFF was found to be efficient in separation of tumor cells from healthy blood cells [38], and for separation of electroporated cells from non-porated ones [97].
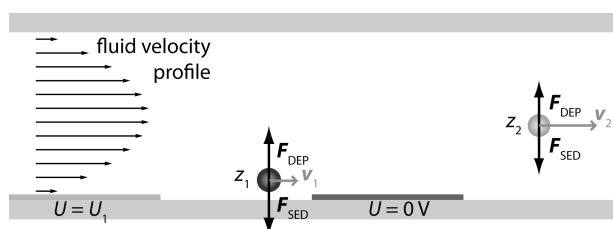

Figure 10: Dielectrophoretic field-flow fractionation

An alternative to metal microelectrodes is to use arrays of insulator structures to locally distort an otherwise homogeneous electrical field. In this technique, known as insulator dielectrophoresis (iDEP), metal macroelectrodes such as wire rods or machined metal plates are used to create a homogeneous electric field across an array of insulator structures. The insulator structures distort the field, creating its gradient. Glass, polymers or carbon can be used as insulator structures. The advantages are lower cost of fabrication and reduced metal-liquid interface effects, but as interelectode distances are in the range of millimeters, a rather higher voltage is required for efficient separation [82].

Macroelectrodes can also be positioned outside the channel, at its sides, or dipped into the channel at its inlet and outlet, with glass beads used as insulating structures. Channels with etched structures in glass, or structures from polymers provide better conditions for fluid flow. Thus Lapizco-Encinas et al. [98] fabricated an iDEP chamber with a channel 10 μm deep and etched in glass using standard photolithography, wet etching, and bonding techniques. Glass pillars as shown on Figure 8e distort the electric field generated between two platinum wires in channel inlet and outlet, distanced at 1 cm. In this design, the PDMS cover was reversibly bonded to the glass by vacuum. DC electric field with average amplitude up to 200 V/cm was used for trapping living bacteria, while dead bacteria passed through the channel untrapped.

iDEP devices have small surface of metal electrodes comparing to classical electrodes. Further modification of iDEP is contactless DEP (cDEP), where electrodes are insulated from cell suspension by a thin layer of PDMS [2], [99]. Channels filled with high conductive phosphate buffer saline form the electrodes (Figure 8e). Advantage of insulated electrodes are no contamination with metal ions, no bubble formation, and inexpensive fabrication suitable for disposable devices. These devices were used for characterisation of mouse ovaian cancer cells in different stages of cancere progression [76] and separation of tumor initiating cells from a population of human prostate cancer cells (PC3) [100].

Detection and separation of tumor initiating cells raised attention in the last years, since many people are diagnosed with cancer in late stages. Detection of tumor initiating cells using surface biomarkers is not reliable and too expensive for screening of large population of patients [101], howerer DEP is one of the methods thst allow for identification or/and separation of tumor initiating cells just by electrical properties without using any fluorescent markers [38], [100], [102], [103].

4.6 Cell patterning

DEP can be used for controlable patterning of biomaterials and bioactive structures for the formation of tissues and tissue-like structures [16].

It can be used for formation of cells to form artificial skin Yusvana at al. [104] fabricated interdigitated and castellated electrodes on ITO-covered glass to pattern skin cells to form artificial skin. Cells are collected between the electrodes and held for 10 min to adhere to each other. Fibrinogen and thrombin solution is added to atherent cells for further immobilisation. Xu et al. [105] designed a chip for dielectrophoretic patterning cells in micro-wells where they can be electroporated. Chamber

is constructed of bottom glass with gold electrodes and top cover glass with ITO electrode. For heterotypic cell positioning, different types of cells are separately introduced into the device, and the electrodes are selectively energized to trap different cells. Trapped cells can be electroporated and transfected with different plasmids.

4.7 Cell fusion

Both in conventional and microfluidic applications, cell fusion is a two-steps procedure. First, the cells are brought into close contact, typically achieved by dielectrophoretic force (generated either by shaping of the electrodes, or by placement of insulating structures into the channel). Second, strong electric pulses are delivered, causing the cells to electroporate and thus reach a fusogenic state. The use of the same electrodes for the two purposes simplifies the design, yet hampers the efficiency, as for dielectrophoretic alignment the field must be nonhomogeneous, while for electrofusion a homogeneous field is preferable, as to avoid both the irreversible electroporation of the cells that are exposed to a field too strong, and the lack of fusogenic state inducement in the cells that are exposed to a field that is too weak.

The first microfluidic chamber for cell electrofusion had two wire electrodes on a glass 0.1 to 0.2 mm apart, using positive dielectrophoresis to bring the cells into close contact before applying strong electric pulses that induced fusion [32]. Many adaptations of this design were published since [106].

The most typical shape of electrodes is castellated. Ju et al. [107] fabricated a chamber with thin Ti-Au electrodes, which are fabricated with standard soft lithography. Channels with fluidic ports are fabricated of PDMS. Cover can be opened, allowing for removal of fused cells with a pipette. Alignment of various plant cells was successful and yield of fused cells was 3-5 %, which is relatively low.

Electrodes thicker than the cell diameter offer highly controlled exposure of cells to electric field. Cao et al. [108] thus fabricated castellated gold electrodes 20 μm thick on silicon, with fabrication steps shown in Figure 11. Channels were etched in silicon wafer, followed by oxidation, titanium sputtering and etching, and gold sputtering and etching. Distance between two counter-electrodes in different chambers varied from 50 to 100 μm. For cell alignment, they used 1-4 MHz sine AC voltage, followed by electroporative DC pulses with electric field amplitudes ranging from 1 to 10 kV/cm, and a damped sine voltage delivered after the pulses to retain the contact between adjacent cells. For plant protoplasts, fusion efficiency of up to 44 % was obtained.
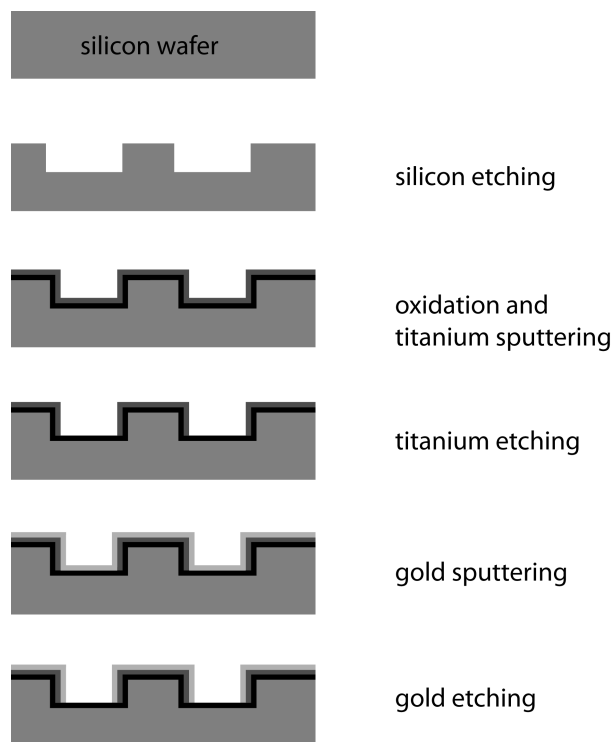

Figure 11: Fabrication steps of thick electrodes. Adapted from [108].

Hu at al. developed two types of thick castellated electrodes [48], [109]. Their first device was fabricated on silicon on an insulating substrate. A layer of highly doped silicon 40 μm thick served as vertical sidewalls of the microfluidic channel. On top of this layer, a thin aluminum film was deposited, patterned and etched by inductively coupled plasma etching. A film of SiO_2 was deposited on the fabricated surface using plasma-enhanced chemical vapor deposition, the unwanted SiO_2 was etched away, and then after another photolithography, channels were etched into the silicon. A PDMS cover with fluidic ports was bonded on the top to form a microfluidic channel. The shortest distance between electrodes was 60 μm, and 2-5 V at 1 MHz was used for dielectrophoretic cell alignment of HEK-293 cells and tobacco leaf protoplasts. The fusion efficiency of 40 % was obtained with a throughput of about 400 fused cells per hour in one channel.

Their second electrofusion chip consisted of a serpentine-shaped microchannel integrated with three-dimensional, thin-film microelectrode arrays fabricated on quartz glass substrate, and with a PDMS cover. The height of the channel was 25 μm and the distance between electrodes 80 μm. A thin film layers of titanium and gold were deposited on glass and patterned with standard lithography technology. A 40 μm thick Durimide 7510 layer was stacked onto the pattern obtained from the previous step, and the pattern of the microchannel was formed by standard lithography. The wafer

was then cured at a high temperature. During the curing procedure, the thickness of Durimide was reduced to 25 μm and the sidewalls reached a 65° inclination. A layer of resist was then deposited and patterned to protect the bottom of the channel, and finally a 300 nm film of gold was sputtered by a magnetron, and the unwanted gold was washed with acetone. In this manner, the three-dimensional microelectrode structure wrapping around the microchannel wall was formed. The chip was tested with K562 cells, which were dielectrophoretically aligned and then electroporated in the same manner as described above, yielding an average fusion efficiency of 43 %.
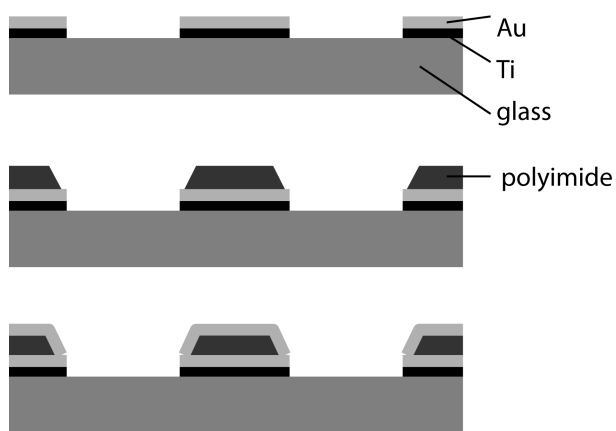

Figure 12: Basic schematics of fabrication steps of thick electrodes with gold layer over patterned polyimide Durimide 7510. Adapted from [48].

For most applications of cell fusion, the cells have to fuse pairwise, since multinucleate cells are typically not viable, and the two cells forming the fusing pair have to belong to two different types, so that the fused hybrid acquires the properties of both these types. In contrast, clustering of cells on simple microelectrodes is largely random, with fusion yielding many multi-cell and single-type hybrids. To improve the yield of the paired two-types hybrids, special structures are introduced into the microfluidic channels, and special protocols are developed.

Skeley et al. [110] thus fabricated a microfluidic device with thousands of single-cell traps formed as cup-shaped indentations in structures made of PDMS. The master for PDMS molding was made of SU-8, the electrodes were fabricated on glass slides from a thin film of chromium and then bonded with PDMS. The pairing of cells of two different types was achieved in three steps as shown on Figure 13. First, the cells were pumped through the chamber, getting trapped in the shallow cup-shaped traps. Second, the direction of flow was reversed, forcing the trapped cells to move directly into the deeper cup-shaped traps located on the opposite side of each trapping structure. Finally, another

population of cells was loaded as to fill the remaining place in deeper cups, so that the formed cell pairs consisted of the two different types of cells. The cells were then electroporated by 50 μs pulses with amplitudes between 0.5 and 2 kV/cm. The pairing efficiency was about 70 %, and more than 50 % of all the cells were paired properly and fused.

Kemna et al. [111] used a similar approach and fabrication technique. With NS-1 and CD19+ B-cells, they obtained a fusion efficiency of about 50%, with a 1 % yield of functional hybridoma, which was considerably higher than the yield of the same hybridoma they were able to achieve by bulk electrofusion.
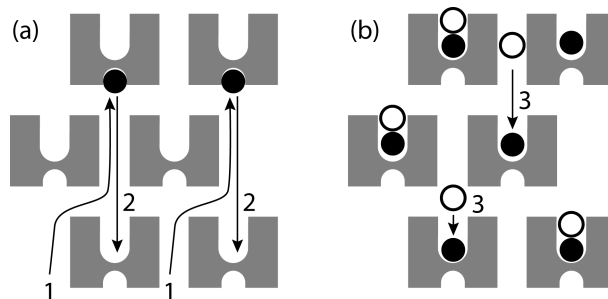

Figure 13: Cell electrofusion; (a) trapping of cells in small cups, reversing fluid flow and moving/shifting cells to large cups, (b) adding second type of cells, electroporation and cell fusion. Adapted from [110].

Another possibility for attaining a dielectrophoretic alignment of cells are insulating structures that concentrate the electric field. Masuda et al. [112] developed a microfluidic chip with two channels separated by a dielectric structure that allowed them to bring together a pair of cells of two different types, and then to electroporate and fuse them (Figure 14).
Mottet et al. [113] modified this design by enlarging the holes so that the fused cells could freely float through the channel, with the chip fabricated on a glass substrate. The dielectric structure separating the two channels had a thickness of 30 μm and a width of either 20 or 30 μm. One hole was about 30 μm wide and allowed for the focusing of the electric field. Thin gold electrodes were fabricated using a lift-off technique, and a thick SU-8 mold was formed on these thin electrodes as to form thick electrodes by electrodeposition (copper electroplating from sulfuric acid solution). SU-8 was then removed and a new layer of SU-8 deposited to form the walls of a channel. The channel was closed by bonding a dry SU-8 film and finally sealed by bonding a glass cover with fluid connectors. The glass cover of the chip allowed to monitor the cells being electrofused under a microscope.
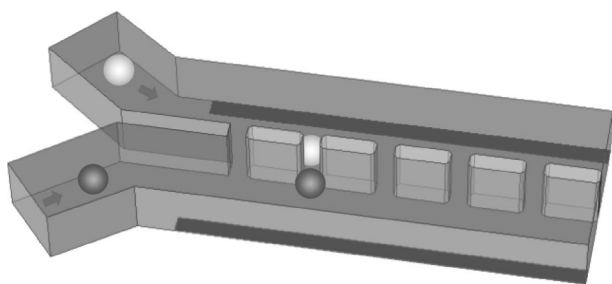
Figure 14: Electrofusion in a chamber with two channels separated by dielectric structures. Adapted from [113].

5 Conclusions

During the last two decades, many microfluidic devices for exposure of cells to electric field have been developed. They are typically made either on glass wafers with standard soft lithography, or out of inexpensive plastics such as PDMS, which can be replaced for every experiment. Among the advantages of small microfluidic devices, as opposed to larger bulk devices, are the highly controllable electric field, lower voltage on the electrodes, faster heat dissipation, small volume of reagents used, and *in situ* observation of the cell response. Still, current chambers are generally difficult to use and require external devices for operation. Compatibilization among these devices and their integration into purely microfluidic setups is expected to add considerable further value to the concept of an integrated *lab-on-a-chip*.

Acknowledgement

References

1. J. Chen, J. Li, and Y. Sun, "Microfluidic approaches for cancer cell detection, characterization, and separation," Lab on a Chip, vol. 12, no. 10, p. 1753, 2012.
2. H. Shafiee, J. Caldwell, M. Sano, and R. Davalos, "Contactless dielectrophoresis: a new technique for cell manipulation," Biomed. Microdevices, vol. 11, no. 5, pp. 997–1006, 2009.
3. C. Liu, T. Stakenborg, S. Peeters, and L. Lagae, "Cell manipulation with magnetic particles toward microfluidic cytometry," Journal of Applied Physics, vol. 105, no. 10, p. 102014, 2009.
4. D.-H. Kim, P. K. Wong, J. Park, A. Levchenko, and Y. Sun, "Microengineered Platforms for Cell Mechanobiology," Annual Review of Biomedical Engineering, vol. 11, pp. 203–233, 2009.
5. M. Ni, W. H. Tong, D. Choudhury, N. A. A. Rahim, C. Iliescu, and H. Yu, "Cell Culture on MEMS Platforms: A Review," International Journal of Molecular Sciences, vol. 10, no. 12, pp. 5411–5441, 2009.
6. D. Mark, S. Haeberle, G. Roth, F. von Stetten, and R. Zengerle, "Microfluidic lab-on-a-chip platforms: requirements, characteristics and applications," Chem. Soc. Rev., vol. 39, no. 3, pp. 1153–1182, 2010.
7. E. Brouzes, M. Medkova, N. Savenelli, D. Marran, M. Twardowski, J. B. Hutchison, J. M. Rothberg, D. R. Link, N. Perrimon, and M. L. Samuels, "Droplet microfluidic technology for single-cell high-throughput screening," Proc. Natl. Acad. Sci. U. S. A., vol. 106, no. 34, pp. 14195–14200, 2009.
8. B. Eker, R. Meissner, A. Bertsch, K. Mehta, and P. Renaud, "Label-Free Recognition of Drug Resistance via Impedimetric Screening of Breast Cancer Cells," PLoS ONE, vol. 8, no. 3, p. e57423, 2013.
9. J. Hong, J. B. Edel, and A. J. deMello, "Micro- and nanofluidic systems for high-throughput biological screening," Drug Discovery Today, vol. 14, no. 3–4, pp. 134–146, 2009.
10. M.-H. Wu, S.-B. Huang, and G.-B. Lee, "Microfluidic cell culture systems for drug research," Lab Chip, vol. 10, no. 8, pp. 939–956, 2010.
11. R. N. Zare and S. Kim, "Microfluidic platforms for single-cell analysis," Annu. Rev. Biomed. Eng., vol. 12, pp. 187–201, 2010.
12. P. Tathireddy, Y.-H. Choi, and M. Skliar, "Particle AC electrokinetics in planar interdigitated microelectrode geometry," J. Electrostat., vol. 66, no. 11–12, pp. 609–619, 2008.
13. Q. Guan, S. D. Noblitt, and C. S. Henry, "Electrophoretic separations in poly(dimethylsiloxane) microchips using a mixture of ionic and zwitterionic surfactants," Electrophoresis, vol. 33, no. 2, pp. 379–387, 2012.
14. H. A. Pohl and J. S. Crane, "Dielectrophoresis of cells," Biophys. J., vol. 11, no. 9, pp. 711–727, 1971.
15. L.-S. Jang, P.-H. Huang, and K.-C. Lan, "Single-cell trapping utilizing negative dielectrophoretic quadrupole and microwell electrodes," Biosensors and Bioelectronics, vol. 24, no. 12, pp. 3637–3644, 2009.

16. Z. R. Gagnon, "Cellular dielectrophoresis: Applications to the characterization, manipulation, separation and patterning of cells," Electrophoresis, vol. 32, no. 18, pp. 2466–2487, 2011.

17. M. M. Meighan, S. J. R. Staton, and M. A. Hayes, "Bioanalytical separations using electric field gradient techniques," Electrophoresis, vol. 30, no. 5, pp. 852–865, 2009.

18. P. Patel and G. H. Markx, "Dielectric measurement of cell death," Enzyme Microb. Technol., vol. 43, no. 7, pp. 463–470, 2008.

19. T. B. Jones, "Basic theory of dielectrophoresis and electrorotation," IEEE Eng. Med. Biol. Mag., vol. 22, no. 6, pp. 33–42, 2003.

20. J. Voldman, "Electrical forces for microscale cell manipulation," Annu. Rev. Biomed. Eng., vol. 8, pp. 425–454, 2006.

21. E. Neumann and K. Rosenheck, "Permeability changes induced by electric impulses in vesicular membranes," J. Membrane Biol., vol. 10, pp. 279–290, 1972.

22. J. Weaver and Y. Chizmadzhev, "Theory of electroporation: A review," Bioelectrochem. Bioenerg., vol. 41, no. 2, pp. 135–160, 1996.

23. J. C. Weaver, "Electroporation of biological membranes from multicellular to nano scales," IEEE Trans. Dielect. Electr. Insul., vol. 10, no. 5, pp. 754–768, 2003.

24. T. Kotnik, P. Kramar, G. Pucihar, D. Miklavčič, and M. Tarek, "Cell membrane electroporation- Part 1: The phenomenon," IEEE Electrical Insulation Magazine, vol. 28, no. 5, pp. 14–23, 2012.

25. G. Serša, D. Miklavčič, M. Čemažar, Z. Rudolf, G. Pucihar, and M. Snoj, "Electrochemotherapy in treatment of tumours," Eur. J. Surg. Oncol., vol. 34, no. 2, pp. 232–240, 2008.

26. A. Gothelf and J. Gehl, "Gene Electrotransfer to Skin; Review of Existing Literature and Clinical Perspectives," Curr. Gene Ther., vol. 10, no. 4, pp. 287–299, 2010.

27. E. W. Lee, S. Thai, and S. T. Kee, "Irreversible electroporation: a novel image-guided cancer therapy," Gut Liver, vol. 4 Suppl 1, pp. 99–104, 2010.

28. M. Sack, J. Sigler, S. Frenzel, C. Eing, J. Arnold, T. Michelberger, W. Frey, F. Attmann, L. Stukenbrock, and G. Müller, "Research on Industrial-Scale Electroporation Devices Fostering the Extraction of Substances from Biological Tissue," Food Eng. Rev., vol. 2, no. 2, pp. 147–156, 2010.

29. M. Morales-de la Peña, P. Elez-Martínez, and O. Martín-Belloso, "Food preservation by pulsed electric fields: an engineering perspective," Food Eng. Rev., vol. 3, pp. 94–107, 2011.

30. T. Kotnik, F. Bobanović, and D. Miklavčič, "Sensitivity of transmembrane voltage induced by applied electric fields - a theoretical analysis," Bioelectrochem Bioenerg, vol. 43, no. 2, pp. 285–291, 1997.

31. D. Miklavčič and M. Puc, "Electroporation," in Wiley encyclopedia of biomedical engineering, M. Akay, Ed. Hoboken: Wiley-Interscience, 2006.

32. U. Zimmermann, "Electric field-mediated fusion and related electrical phenomena," Biochimica et Biophysica Acta (BBA) - Reviews on Biomembranes, vol. 694, no. 3, pp. 227–277, 1982.

33. M. Ušaj, K. Trontelj, R. Hudej, M. Kandušer, and D. Miklavčič, "Cell size dynamics and viability of cells exposed to hypotonic treatment and electroporation for electrofusion optimization," Radiol. Oncol., vol. 43, no. 2, pp. 108–119, 2009.

34. M. Ušaj, K. Trontelj, D. Miklavčič, and M. Kandušer, "Cell–cell electrofusion: optimization of electric field amplitude and hypotonic treatment for Mouse melanoma (B16-F1) and Chinese hamster ovary (CHO) cells," J. Membrane Biol., vol. 236, no. 1, pp. 107–116, 2010.

35. T. R. Hsu, MEMS and microsystems : design, manufacture, and nanoscale engineering, 2nd ed. John Wiley & Sons, 2008.

36. F. Chollet and H. Liu, A (not so) short introduction to Micro Electro Mechanical Systems, 3.0 ed. Singapore, 2009.

37. H. Becker and C. Gärtner, "Polymer microfabrication technologies for microfluidic systems," Analytical and Bioanalytical Chemistry, vol. 390, no. 1, pp. 89–111, 2007.

38. P. R. C. Gascoyne, J. Noshari, T. J. Anderson, and F. F. Becker, "Isolation of rare cells from cell mixtures by dielectrophoresis," Electrophoresis, vol. 30, no. 8, pp. 1388–1398, 2009.

39. B.-H. Jo, L. M. Van Lerberghe, K. M. Motsegood, and D. J. Beebe, "Three-dimensional micro-channel fabrication in polydimethylsiloxane (PDMS) elastomer," Journal of Microelectromechanical Systems, vol. 9, no. 1, pp. 76–81, 2000.

40. T. Tomov and I. Tsoneva, "Are the stainless steel electrodes inert?," Bioelectrochemistry, vol. 51, no. 2, pp. 207–209, 2000.

41. T. Kotnik, D. Miklavčič, and L. M. Mir, "Cell membrane electropermeabilization by symmetrical bipolar rectangular pulses - Part II. Reduced electrolytic contamination," Bioelectrochemistry, vol. 54, no. 1, pp. 91–95, 2001.

42. U. Friedrich, N. Stachowicz, A. Simm, G. Fuhr, K. Lucas, and U. Zimmermann, "High efficiency electrotransfection with aluminum electrodes using microsecond controlled pulses," Bioelectrochemistry and Bioenergetics, vol. 47, no. 1, pp. 103–111, 1998.

43. F. E. H. Tay, L. M. Yu, A. J. Pang, and C. Iliescu, "Electrical and thermal characterization of a dielectrophoretic chip with 3D electrodes for cells ma-

nipulation," Electrochim. Acta, vol. 52, no. 8, pp. 2862–2868, 2007.

44. H. Cong and T. Pan, "Microfabrication of conductive PDMS on flexible substrates for biomedical applications," in Nano/Micro Engineered and Molecular Systems, 2009. NEMS 2009. 4th IEEE International Conference on, 2009, pp. 731 –734.

45. X. Z. Niu, S. L. Peng, L. Y. Liu, W. J. Wen, and P. Sheng, "Characterizing and Patterning of PDMS-Based Conducting Composites," Adv. Mater., vol. 19, no. 18, pp. 2682–2686, 2007.

46. A. N. K. Lau, A. T. Ohta, H. L. Phan, H.-Y. Hsu, A. Jamshidi, P.-Y. Chiou, and M. C. Wu, "Antifouling coatings for optoelectronic tweezers," Lab Chip, vol. 9, no. 20, p. 2952, 2009.

47. C. Iliescu, L. M. Yu, G. L. Xu, and F. E. H. Tay, "A dielectrophoretic chip with a 3-D electric field gradient," J. Microelectromech. Syst., vol. 15, no. 6, pp. 1506–1513, 2006.

48. N. Hu, J. Yang, S. Qian, S. W. Joo, and X. Zheng, "A cell electrofusion microfluidic device integrated with 3D thin-film microelectrode arrays," Biomicrofluidics, vol. 5, no. 3, pp. 034121–034121–12, 2011.

49. C.-P. Jen and H.-H. Chang, "A handheld preconcentrator for the rapid collection of cancerous cells using dielectrophoresis generated by circular microelectrodes in stepping electric fields," Biomicrofluidics, vol. 5, p. 034101, 2011.

50. P. Sabounchi, A. M. Morales, P. Ponce, L. P. Lee, B. A. Simmons, and R. V. Davalos, "Sample concentration and impedance detection on a microfluidic polymer chip," Biomed Microdevices, vol. 10, no. 5, pp. 661–670, 2008.

51. A. T. Ohta, P. Y. Chiou, H. L. Phan, S. W. Sherwood, J. M. Yang, A. N. K. Lau, H. Y. Hsu, A. Jamshidi, and M. C. Wu, "Optically controlled cell discrimination and trapping using optoelectronic tweezers," IEEE J. Sel. Top. Quantum Electron., vol. 13, no. 2, pp. 235–243, 2007.

52. M. B. Fox, D. C. Esveld, A. Valero, R. Luttge, H. C. Mastwijk, P. V. Bartels, A. van den Berg, and R. M. Boom, "Electroporation of cells in microfluidic devices: a review," Anal. Bioanal.Chem., vol. 385, no. 3, pp. 474–485, 2006.

53. S. K. Kim, J. H. Kim, K. P. Kim, and T. D. Chung, "Continuous Low-Voltage dc Electroporation on a Microfluidic Chip with Polyelectrolytic Salt Bridges," Anal. Chem., vol. 79, no. 20, pp. 7761–7766, 2007.

54. W. G. Lee, U. Demirci, and A. Khademhosseini, "Microscale electroporation: challenges and perspectives for clinical applications," Integr. Biol., vol. 1, no. 3, pp. 242–251, 2009.

55. W. Longsine-Parker, H. Wang, C. Koo, J. Kim, B. Kim, A. Jayaraman, and A. Han, "Microfluidic electro-sonoporation: a multi-modal cell poration methodology through simultaneous application of electric field and ultrasonic wave," Lab Chip, vol. 13, no. 11, pp. 2144–2152, 2013.

56. M. Shahini and J. T. W. Yeow, "Cell electroporation by CNT-featured microfluidic chip," Lab Chip, vol. 13, no. 13, pp. 2585–2590, 2013.

57. A. Adamo, A. Arione, A. Sharei, and K. F. Jensen, "Flow-Through Comb Electroporation Device for Delivery of Macromolecules," Anal. Chem., vol. 85, no. 3, pp. 1637–1641, 2013.

58. D. Selmeczi, T. S. Hansen, Ö. Met, I. M. Svane, and N. B. Larsen, "Efficient large volume electroporation of dendritic cells through micrometer scale manipulation of flow in a disposable polymer chip," Biomedical Microdevices, vol. 13, no. 2, pp. 383–392, 2011.

59. J. Kim, I. Hwang, D. Britain, T. D. Chung, Y. Sun, and D.-H. Kim, "Microfluidic approaches for gene delivery and gene therapy," Lab Chip, vol. 11, no. 23, pp. 3941–3948, 2011.

60. A. Valero, J. N. Post, J. W. van Nieuwkasteele, P. M. ter Braak, W. Kruijer, and A. van den Berg, "Gene transfer and protein dynamics in stem cells using single cell electroporation in a microfluidic device," Lab Chip, vol. 8, no. 1, pp. 62–67, 2008.

61. S. Vassanelli, L. Bandiera, M. Borgo, G. Cellere, L. Santoni, C. Bersani, M. Salamon, M. Zaccolo, L. Lorenzelli, S. Girardi, M. Maschietto, M. Dal Maschio, and A. Paccagnella, "Space and time-resolved gene expression experiments on cultured mammalian cells by a single-cell electroporation microarray," N Biotechnol, vol. 25, no. 1, pp. 55–67, 2008.

62. J. A. Kim, K. Cho, Y. S. Shin, N. Jung, C. Chung, and J. K. Chang, "A multi-channel electroporation microchip for gene transfection in mammalian cells," Biosens. Bioelectron., vol. 22, no. 12, pp. 3273–3277, 2007.

63. H. Y. Wang and C. Lu, "Electroporation of mammalian cells in a microfluidic channel with geometric variation," Anal. Chem., vol. 78, no. 14, pp. 5158–5164, 2006.

64. Y. Zhan, Z. Cao, N. Bao, J. Li, J. Wang, T. Geng, H. Lin, and C. Lu, "Low-frequency ac electroporation shows strong frequency dependence and yields comparable transfection results to dc electroporation," J. Control. Release, vol. 160, no. 3, pp. 570–576, 2012.

65. Y.-C. Lin, C.-M. Jen, M.-Y. Huang, C.-Y. Wu, and X.-Z. Lin, "Electroporation microchips for continuous gene transfection," Sensors and Actuators B: Chemical, vol. 79, no. 2–3, pp. 137–143, 2001.

66. Y. Zhan, J. Wang, N. Bao, and C. Lu, "Electroporation of Cells in Microfluidic Droplets," Analytical Chemistry, vol. 81, no. 5, pp. 2027–2031, 2009.

67. L. A. MacQueen, M. D. Buschmann, and M. R. Wertheimer, "Gene delivery by electroporation after dielectrophoretic positioning of cells in a non-uniform electric field," Bioelectrochemistry, vol. 72, no. 2, pp. 141–148, 2008.

68. Y. Huang and B. Rubinsky, "Microfabricated electroporation chip for single cell membrane permeabilization," Sens. Actuators A Phys, vol. 89, no. 3, pp. 242–249, 2001.

69. H. Lu, M. A. Schmidt, and K. F. Jensen, "A microfluidic electroporation device for cell lysis," Lab Chip, vol. 5, no. 1, pp. 23–29, 2005.

70. H. Sedgwick, F. Caron, P. B. Monaghan, W. Kolch, and J. M. Cooper, "Lab-on-a-chip technologies for proteomic analysis from isolated cells," J. R. Soc. Interface, vol. 5, pp. S123–S130, 2008.

71. C. de la Rosa, P. A. Tilley, J. D. Fox, and K. V. I. Kaler, "Microfluidic Device for Dielectrophoresis Manipulation and Electrodisruption of Respiratory Pathogen Bordetella pertussis," IEEE Transactions on Biomedical Engineering, vol. 55, no. 10, pp. 2426 –2432, 2008.

72. T. Müller, G. Gradl, S. Howitz, S. Shirley, T. Schnelle, and G. Fuhr, "A 3-D microelectrode system for handling and caging single cells and particles," Biosens. Bioelectron., vol. 14, no. 3, pp. 247–256, 1999.

73. E. G. Cen, C. Dalton, Y. Li, S. Adamia, L. M. Pilarski, and K. V. I. S. Kaler, "A combined dielectrophoresis, traveling wave dielectrophoresis and electrorotation microchip for the manipulation and characterization of human malignant cells," J. Microbiol. Methods, vol. 58, no. 3, pp. 387–401, 2004.

74. B. G. Hawkins, C. Huang, S. Arasanipalai, and B. J. Kirby, "Automated dielectrophoretic characterization of Mycobacterium smegmatis," Anal. Chem., vol. 83, no. 9, pp. 3507–3515, 2011.

75. P. R. C. Gascoyne, S. Shim, J. Noshari, F. F. Becker, and K. Stemke-Hale, "Correlations between the dielectric properties and exterior morphology of cells revealed by dielectrophoretic field-flow fractionation," Electrophoresis, vol. 34, no. 7, pp. 1042–1050, 2013.

76. A. Salmanzadeh, M. B. Sano, R. C. Gallo-Villanueva, P. C. Roberts, E. M. Schmelz, and R. V. Davalos, "Investigating dielectric properties of different stages of syngeneic murine ovarian cancer cells," Biomicrofluidics, vol. 7, no. 1, 2013.

77. D. R. Gossett, W. M. Weaver, A. J. Mach, S. C. Hur, H. T. K. Tse, W. Lee, H. Amini, and D. Di Carlo, "Label-free cell separation and sorting in microfluidic systems," Anal Bioanal Chem, vol. 397, no. 8, pp. 3249–3267, 2010.

78. G. Xu, F. E. H. Tay, G. Tresset, F. S. Iliescu, A. Avram, and C. Iliescu, "Recent trends in dielectrophoresis," Inform. Midem, vol. 40, no. 4, pp. 253–262, 2010.

79. K. Khoshmanesh, S. Nahavandi, S. Baratchi, A. Mitchell, and K. Kalantar-zadeh, "Dielectrophoretic platforms for bio-microfluidic systems," Biosens. Bioelectron., vol. 26, no. 5, pp. 1800–1814, 2011.

80. L. Yang, "A review of multifunctions of dielectrophoresis in biosensors and biochips for bacteria detection," Anal. Lett., vol. 45, no. 2–3, pp. 187–201, 2012.

81. L. A. Macqueen, M. Thibault, M. D. Buschmann, and M. R. Wertheimer, "Electro-manipulation of biological cells in microdevices," IEEE Transactions on Dielectrics and Electrical Insulation, vol. 19, no. 4, pp. 1261 –1268, 2012.

82. R. Martinez-Duarte, "Microfabrication technologies in dielectrophoresis applications—A review," Electrophoresis, vol. 33, no. 21, pp. 3110–3132, 2012.

83. P. R. C. Gascoyne, X. B. Wang, Y. Huang, and F. F. Becker, "Dielectrophoretic separation of cancer cells from blood," IEEE Trans. Ind. Appl., vol. 33, no. 3, pp. 670–678, 1997.

84. G. H. Markx, R. Pethig, and J. Rousselet, "The dielectrophoretic levitation of latex beads, with reference to field-flow fractionation," J. Phys. D: Appl. Phys., vol. 30, no. 17, p. 2470, 1997.

85. D. Holmes, N. G. Green, and H. Morgan, "Microdevices for dielectrophoretic flow-through cell separation," IEEE Eng. Med. Biol. Mag., vol. 22, no. 6, pp. 85–90, 2003.

86. J. Oblak, D. Križaj, S. Amon, A. Maček-Lebar, and D. Miklavčič, "Feasibility study for cell electroporation detection and separation by means of dielectrophoresis," Bioelectrochemistry, vol. 71, no. 2, pp. 164–171, 2007.

87. K. Khoshmanesh, C. Zhang, F. Tovar-Lopez, S. Nahavandi, S. Baratchi, A. Mitchell, and K. Kalantar-Zadeh, "Dielectrophoretic-activated cell sorter based on curved microelectrodes," Microfluid. Nanofluid., vol. 9, pp. 411–426, 2010.

88. Aldaeus, Y. Lin, J. Roeraade, and G. Amberg, "Superpositioned dielectrophoresis for enhanced trapping efficiency," Electrophoresis, vol. 26, no. 22, pp. 4252–4259, 2005.

89. J. Voldman, M. Toner, M. L. Gray, and M. A. Schmidt, "Design and analysis of extruded quadrupolar dielectrophoretic traps," J. Electrostat., vol. 57, no. 1, pp. 69–90, 2003.

90. L. S. Wang, L. Flanagan, and A. P. Lee, "Side-wall vertical electrodes for lateral field microfluidic applications," J. Microelectromech. Syst., vol. 16, no. 2, pp. 454–461, 2007.

91. E. B. Cummings and A. K. Singh, "Dielectrophoresis in microchips containing arrays of insulating posts: Theoretical and experimental results," Anal. Chem., vol. 75, no. 18, pp. 4724–4731, 2003.

92. R. S. W. Thomas, P. D. Mitchell, R. O. C. Oreffo, and H. Morgan, "Trapping single human osteoblast-like cells from a heterogeneous population using a dielectrophoretic microfluidic device," Biomicrofluidics, vol. 4, no. 2, p. 022806, 2010.

93. K.-H. Han and A. B. Frazier, "Lateral-driven continuous dielectrophoretic microseparators for blood cells suspended in a highly conductive medium," Lab Chip, vol. 8, no. 7, p. 1079, 2008.

94. N. Lewpiriyawong, K. Kandaswamy, C. Yang, V. Ivanov, and R. Stocker, "Microfluidic characterization and continuous separation of cells and particles using conducting poly(dimethyl siloxane) electrode induced alternating current-dielectrophoresis," Anal. Chem., vol. 83, no. 24, pp. 9579–9585, 2011.

95. Y. Huang, X. B. Wang, F. F. Becker, and P. R. C. Gascoyne, "Introducing dielectrophoresis as a new force field for field-flow fractionation," Biophys. J., vol. 73, no. 2, pp. 1118–1129, 1997.

96. J. Čemažar, D. Vrtačnik, S. Amon, and T. Kotnik, "Dielectrophoretic field-flow microchamber for separation of biological cells based on their electrical properties," IEEE Trans. Nanobiosci., vol. 10, no. 1, pp. 36–43, 2011.

97. J. Čemažar and T. Kotnik, "Dielectrophoretic field-flow fractionation of electroporated cells," Electrophoresis, vol. 33, no. 18, pp. 2867–2874, 2012.

98. B. H. Lapizco-Encinas, R. V. Davalos, B. A. Simmons, E. B. Cummings, and Y. Fintschenko, "An insulator-based (electrodeless) dielectrophoretic concentrator for microbes in water," J. Microbiol. Methods, vol. 62, no. 3, pp. 317–326, 2005.

99. M. B. Sano, J. L. Caldwell, and R. V. Davalos, "Modeling and development of a low frequency contactless dielectrophoresis (cDEP) platform to sort cancer cells from dilute whole blood samples," Biosens. Bioelectron., vol. 30, no. 1, pp. 13–20, 2011.

100. A. Salmanzadeh, L. Romero, H. Shafiee, R. C. Gallo-Villanueva, M. A. Stremler, S. D. Cramer, and R. V. Davalos, "Isolation of prostate tumor initiating cells (TICs) through their dielectrophoretic signature," Lab on a Chip, vol. 12, no. 1, pp. 182–189, 2012.

101. C. Yu, Z. Yao, J. Dai, H. Zhang, J. Escara-Wilke, X. Zhang, and E. T. Keller, "ALDH Activity Indicates Increased Tumorigenic Cells, But Not Cancer Stem Cells, in Prostate Cancer Cell Lines," In Vivo, vol. 25, no. 1, pp. 69–76, 2011.

102. S. Shim, K. Stemke-Hale, A. M. Tsimberidou, J. Noshari, T. E. Anderson, and P. R. C. Gascoyne, "Antibody-independent isolation of circulating tumor cells by continuous-flow dielectrophoresis," Biomicrofluidics, vol. 7, no. 1, pp. 011807–011807–12, 2013.

103. V. Tirino, V. Desiderio, F. Paino, A. D. Rosa, F. Papaccio, M. L. Noce, L. Laino, F. D. Francesco, and G. Papaccio, "Cancer stem cells in solid tumors: an overview and new approaches for their isolation and characterization," FASEB J, vol. 27, no. 1, pp. 13–24, 2013.

104. R. Yusvana, D. J. Headon, and G. H. Markx, "Creation of arrays of cell aggregates in defined patterns for developmental biology studies using dielectrophoresis," Biotechnology and Bioengineering, vol. 105, no. 5, pp. 945–954, 2010.

105. Y. Xu, H. Yao, L. Wang, W. Xing, and J. Cheng, "The construction of an individually addressable cell array for selective patterning and electroporation," Lab on a Chip, vol. 11, no. 14, p. 2417, 2011.

106. N. Hu, J. Yang, S. W. Joo, A. N. Banerjee, and S. Qian, "Cell electrofusion in microfluidic devices: A review," Sensors and Actuators B: Chemical, vol. 178, pp. 63–85, 2013.

107. J. Ju, J.-M. Ko, H.-C. Cha, J. Y. Park, C.-H. Im, and S.-H. Lee, "An electrofusion chip with a cell delivery system driven by surface tension," J. Micromech. Microeng., vol. 19, no. 1, p. 015004, Jan. 2009.

108. Y. Cao, J. Yang, Z. Q. Yin, H. Y. Luo, M. Yang, N. Hu, D. Q. Huo, C. J. Hou, Z. Z. Jiang, R. Q. Zhang, R. Xu, and X. L. Zheng, "Study of high-throughput cell electrofusion in a microelectrode-array chip," Microfluid. Nanofluid., vol. 5, no. 5, pp. 669–675, 2008.

109. N. Hu, J. Yang, Z.-Q. Yin, Y. Ai, S. Qian, I. B. Svir, B. Xia, J.-W. Yan, W.-S. Hou, and X.-L. Zheng, "A high-throughput dielectrophoresis-based cell electrofusion microfluidic device," Electrophoresis, vol. 32, pp. 2488–2495, 2011.

110. A. M. Skelley, O. Kirak, H. Suh, R. Jaenisch, and J. Voldman, "Microfluidic control of cell pairing and fusion," Nat. Meth., vol. 6, no. 2, pp. 147–152, 2009.

111. E. W. M. Kemna, F. Wolbers, I. Vermes, and A. van den Berg, "On chip electrofusion of single human B cells and mouse myeloma cells for efficient hybridoma generation," Electrophoresis, vol. 32, no. 22, pp. 3138–3146, 2011.

112. S. Masuda, M. Washizu, and T. Nanba, "Novel method of cell fusion in field constriction area in fluid integration circuit," IEEE Transactions on Industry Applications, vol. 25, no. 4, pp. 732 –737, 1989.

113. G. Mottet, B. Le Pioufle, and L. M. Mir, "High-resolution analyses of cell fusion dynamics in a biochip," Electrophoresis, vol. 33, no. 16, pp. 2508–2515, 2012.